Science Translational Medicine
AAAS

Supplementary Materials for

RNF41 orchestrates macrophage-driven fibrosis resolution and hepatic regeneration

Alazne Moreno-Lanceta *et al.*

Corresponding author: Pedro Melgar-Lesmes, pmelgar@ub.edu

Sci. Transl. Med. **15**, eabq6225 (2023)
DOI: 10.1126/scitranslmed.abq6225

The PDF file includes:

Other Supplementary Material for this manuscript includes the following:

Materials and methods

Physicochemical characterization of nanoparticles

Nanoparticle size was determined by dynamic light scattering (DLS), using a Zetasizer nano ZS (Malvern Instruments Ltd). Measurements were carried out at 25 °C and at fixed angle of 173°, by analyzing the intensity of the scattered light supplied by a helium-neon laser (4 mW, λ = 633 nm). DLS data were calculated from the autocorrelation function of scattered light by means of two mathematical approaches: the cumulants method and Dispersion Technology Software nano v. 5.10 (Malvern Instruments Ltd). Through the cumulants analysis, two important parameters were obtained: the mean hydrodynamic diameter (Z-Average) and the width of the particle size distribution (polydispersity index-PDI). To prepare samples for the measurements, 20 μL of graphite nanoparticle suspension were dispersed in 1480 μL of PBS, in an ordinary cuvette. Reported values of Z-Average and PDI corresponded to the average of approximately 40 measurement runs. The size and morphology of different nanoparticles were characterized by TEM, using a JEOL JEM 1010 microscope (JEOL) equipped with an AMT XR40 digital imaging camera, at a magnification of 75000X and a maximum accelerating voltage of 100 kV. Particle diameter was determined in approximately 300 randomly selected nanoparticles from different TEM images using the morphometry software ImageJ v. 1.44 (U.S. National Institutes of Health). Osmolality was determined from osmometric depression of the freezing point (Advanced Instruments Osmometer 3300).

Cell culture

Primary human umbilical vein endothelial cells (HUVECs), mouse macrophages (RAW 264.7) and human monocytes (THP-1) were supplied by ATCC. Human LX-2 hepatic stellate cells were a generous gift from Dr Scott L Friedman. Human macrophages were obtained from incubation of THP-1 with phorbol myristate acetate (PMA) (100 ng/mL) for 2 days. Freshly isolated primary hepatic $CD11b^{+}$-macrophages were obtained from the livers of healthy mice. Dulbecco's phosphate buffered saline (DPBS), Dulbecco's Modified Eagle Medium (DMEM) and penicillin/streptomycin were purchased from Thermo Fisher Scientific Inc. HUVECs were cultured in pre-gelatinized plates with endothelial growth medium (EGM) supplemented with EGM-2 growth supplements (Lonza), 10% fetal bovine serum (FBS), and 50 U/mL

penicillin/streptomycin. HUVECs were passaged when they reached 80% confluence and passages 2–5 were used for all experiments. RAW 264.7 mouse macrophages, isolated mouse hepatocytes, and hepatic stellate cells were cultured with DMEM supplemented with 10% FBS. Isolated mouse hepatic $CD11b^+$-macrophages were cultured with DMEM supplemented with 1% FBS. Human LX-2 cells were cultured with DMEM supplemented with 2% FBS. All cells were grown at 37 °C and 5% CO_2 in a water jacketed incubator.

Prolonged inflammation assay in macrophages

Mouse RAW 264.7 and human THP-1 macrophages were seeded at 2 x 10^4 cell/cm^2 density with complete DMEM medium supplemented with low FBS (1%) and incubated with TNF-α (5 ng/mL, Life Technologies) for 7 days, with daily renovation of this pro-inflammatory medium. Cells were harvested at different time points; at day 0 (16 hours after seeding with no TNF-α stimulation), and 1, 3, 5 and 7 days after TNF-α stimulation for RNA isolation or protein extraction using the TRIZOL kit (Gibco-Invitrogen) or lysis buffer containing 20 mM Tris-HCl, at pH 7.4, 1% Triton X-100, 0.1% SDS, 50 mM NaCl, 2.5 mM EDTA, 1 mM $Na_4P_2O_7$ $10H_2O$, 20 mM NaF, 1 mM Na_3VO_4, 2 mM Pefabloc and a cocktail of protease inhibitors (Complete Mini, Roche) with protease inhibitors (Thermo Fisher, 87786) and phosphatase inhibitors (Thermo Fisher, 78420), respectively, for Real-time PCR and Western blot experiments. Freshly isolated primary hepatic $CD11b^+$-macrophages from healthy male mice were seeded at 2 x 10^4 cell/cm^2 density with complete DMEM medium supplemented with low FBS (1%) and incubated with TNF-α (5 ng/mL, Life Technologies) for 3 days, with daily renovation of this pro-inflammatory medium. Cells were harvested at different time points; at day 0 (16 hours after seeding with no TNF-α stimulation), and 1, 2 and 3 days after TNF-α stimulation for RNA isolation using TRIZOL kit for Real-time PCR.

Biological characterization of nanoparticles

Plasmid-DGNP cytotoxicity was analyzed on HUVECs using the CellTiter 96 Aqueous One Solution Cell Proliferation Assay (MTS assay, Promega). Briefly, cells were seeded in pre-gelatinized 96-well plates at a cell density of 5×10^3 cells per well, serum starved for 6 h and then incubated with plasmid-DGNP at different concentrations (500, 50 and 5 µg/mL) for 24h. Just before determination of cell viability, cells were washed with PBS and transferred into starvation medium. Cytotoxicity was determined by adding 20 µL of MTS solution to each well. After 2 h,

the absorbance was measured at 490 nm using a microplate spectrophotometer (Varioskan Flash spectrophotometer, Thermofisher Scientific). Cell viability was expressed as the absorbance of cells treated with plasmid-DGNP relative to cells treated with PBS (control). Each condition was performed in quadruplicates and reported as mean ± SD.

Uptake kinetics of plasmid-DGNP

RAW 264.7 mouse macrophages were cultured with DMEM with 10% FBS in 24 wells (10^5 cells/well) for 24 hours and then serum-starved for 6 hours. Afterwards cells were incubated with plasmid-DGNP 100 ng/mL in the presence or absence of TNF-α (5 ng/mL) and images were taken at different time points (30, 60, 120 and 180 minutes) with a light microscope. Black aggregates of plasmid-DGNP were visualized at high magnification to establish the number of cells incorporating plasmid-DGNP. Percentage of cells incorporating plasmid-DGNP is calculated with the formula: number of cells with black aggregates/total number of cells per field x 100. At least 30 different fields were used to calculate the uptake percentage per time point.

Intracellular localization of FITC-DGNP in macrophages

DGNP (10 µg/mL) were incubated with FITC (2 mg/mL, Sigma) for 1 h at room temperature in the dark. Afterwards FITC-DGNP were centrifuged at 21000 Gs for 10 min, washed three times with DMSO, and then three times with PBS for subsequent *in vitro* experiments. FITC-DGNP were incubated with inflamed RAW 264.7 mouse macrophages for 24 h, washed with PBS, and visualized with an epifluorescence microscope (Fluo Zeiss Axio Observer Z1, Zeiss) and a digital imaging system (Ret Exi, Explora Nova). DAPI was used as mounting medium to counterstain cell nuclei.

Functional assay of plasmid transfection efficiency and anti-inflammatory subset switch

The transfection efficiency of plasmid-DGNP complexes was studied in inflamed RAW 264.7 macrophages. Cells were seeded at a concentration of 5×10^4 cells in 2-well Labtek II chamber slides, grown to 80% confluence, and inflamed with TNF-α (5 ng/mL) for 16 h. After that, cells were serum-starved for 6 h and incubated for 3 h with 100 ng/mL plasmid-DGNP containing 10 ng/mL of plasmid DNA expressing RNF41 or EGFP reporter. Cells were then washed and incubated for 3 days. Afterwards, cells were washed with PBS and mounted with a coverslip using a DAPI mounting medium to counterstain cell nuclei. Intracellular presence of

synthesized EGFP was visualized with an epifluorescence microscope. To analyze the possible switch from pro-inflammatory to anti-inflammatory macrophages, cells were stained with rabbit polyclonal anti-mannose receptor (1:100, Abcam, ref: ab64693) and revealed with Cy3-conjugated donkey-anti-rabbit IgG (Jackson ImmunoResearch Laboratories, ref: 711-167-003) incubated for 1h at room temperature. The presence of synthesized mannose receptor was visualized with an epifluorescence microscope.

Detection of EGFP fluorescence in liver isolated cells

Hepatic $CD11b^+$-macrophages, hepatocytes and hepatic stellate cells were isolated from the liver of fibrotic mice 24 hours after treatment with pSCR-DGNP as described in the method section. Liver endothelial cells were obtained after MACS-purification with CD31 specific antibodies (Invitrogen, ref: PA5-14372). Hepatocytes, liver endothelial cells and hepatic stellate cells were MACS-purified using negative selection with Ly6G (RyD Systems, ref: 25872-1-AP) and PDCA-1 (Invitrogen, ref: PA5-23505) antibodies linked to anti-rabbit IgG microbeads (Miltenyi Biotec, ref: 130-048-602) and CD11b magnetic beads (Miltenyi Biotec, 130-049-601) to eliminate any contaminating $CD11b^+$ macrophages. Isolated cells fractions were resuspended in 300 µl of lysis buffer containing 20 mM Tris-HCl, at pH 7.4, 1% Triton X-100, 0.1% SDS, 50 mM NaCl, 2.5 mM EDTA. EGFP cell fluorescence of each fraction was measured using 96-well microplate for fluorescence-based assays (Invitrogen) in a microplate fluorescence reader (Tecan Spark 10M Microplate Reader) with the excitation peak at 488 nm and the emission peak at 510 nm. Liver isolated cells from fibrotic animals without pSCR-DGNP treatment were used as control to normalize relative fluorescence units observed in the cells from pSRC-DGNP treated animals. Fluorescence in isolated cells was expressed as relative fluorescence units (RFU) per miligram of cell fraction. Cell protein content was measured using BCA assay kit (Thermo Fisher Scientific Inc).

Proliferation assay in isolated hepatocytes and pro-fibrogenic activation of LX-2 hepatic stellate cells incubated with macrophage-derived conditioned medium

Effects of macrophage-derived conditioned medium from RAW 264.7 macrophages treated with the different plasmid-DGNP were analyzed in mouse isolated hepatocytes using the CellTiter 96 Aqueous One Solution Cell Proliferation Assay (MTS assay, Promega) and in LX-2 hepatic stellate cells. Isolated mouse hepatocytes and LX-2 were seeded in 96-well plates at a cell

density of 5×10^3 cells per well, serum starved for 6 h, washed with PBS and then incubated with fresh starving medium mixed with conditioned medium 1:1 from RAW 264.7 macrophages treated with PBS, 10% FBS, TNF-α only, TNF-α + pScramble-DGNP, TNF-α + pRNF41-DGNP, TNF-α + pshRNF41-DGNP for 3 days. Conditioned medium was centrifuged, and supernatants stored at -80 ºC for proliferation assays. Conditioned medium from macrophages treated with pRNF41-DGNP was mixed with IGF-1 antibody (ABClonal, ref: A0303) (2 µg/mL) for 2 h before the proliferation assay to evaluate its involvement in the proliferation of hepatocytes. Final conditioned medium mixtures were incubated with hepatocytes for 24 h. Proliferation was determined by adding 20 µL of MTS solution to each well. After 2 h, the absorbance was measured at 490 nm using a microplate spectrophotometer (Varioskan Flash spectrophotometer, Thermofisher Scientific). Cell viability was expressed as absorbance and compared to the absorbance of cells receiving an equal volume of PBS (control). LX-2 hepatic stellate cells were resuspended in TRIZOL to isolate RNA for Real-Time PCR of pro-fibrogenic genes. Each condition was performed in sextuplicate and reported as mean ± SD.

Western Blot

Total protein was extracted from cells with lysis buffer containing 20 mM Tris-HCl, at pH 7.4, 1% Triton X-100, 0.1% SDS, 50 mM NaCl, 2.5 mM EDTA, 1 mM $Na_4P_2O_7$ $10H_2O$, 20 mM NaF, 1 mM Na_3VO_4, 2 mM Pefabloc and a cocktail of protease inhibitors (Complete Mini, Roche) and phosphatase inhibitors (Thermo Fisher, 78420). Proteins were separated on a 10% SDS-polyacrylamide gel (Mini Protean III, BioRad) and transferred for 2 hours at 4°C to nitrocellulose membranes of 0,45 µm (Transblot Transfer Medium, BioRad) that were stained with Ponceau-S red as a primary control for protein loading. The membranes were incubated at 4°C overnight with the following antibodies: rabbit anti-pAkt (Ser127) (1:1000, Cell Signaling, ref: 9271) and anti-Akt (1:1000, Cell Signaling, ref: 9272), rabbit anti-phospho-Erk (1:1000, Cell Signaling, ref: 4370S) and anti-Erk (1:1000, Cell Signaling, ref: 4695) and β-actin (1:2000, Cell Signaling, ref: 4970) as loading control. Next, the membranes were incubated with a donkey ECL-anti-rabbit IgG peroxidase-conjugated secondary antibody at 1:2000 dilution (1:2000, Thermo Fisher, ref: SA1-200) for 1 hour at room temperature. The bands were visualized using Chemidoc Imaging System (Biorad Laboratories, Inc) and quantified by computer-assisted densitometry analysis (ImageJ).

Immunofluorescence and imaging in tissues

Liver was excised and tissue was washed with PBS and fixed with 10% buffered formaldehyde solution for 24h. Afterwards the tissue was cryo-protected with 30% sucrose solution (in PBS) and then embedded using Tissue-Tek OCT compound (Sakura Fineteck) and frozen. Liver sections underwent 1% SDS solution antigen retrieval for 5 minutes at room temperature and then were blocked with 5% normal goat serum. Liver sections were incubated with rabbit polyclonal anti-mannose receptor (1:100, Abcam, ref: ab64693), rabbit polyclonal anti-PCNA antibody (1:50, Abcam, ref: ab152112), rat anti-Ly-6C monoclonal IgG antibody (1:100, Thermofisher Scientific, ref: ER-MP20), rabbit anti-iNOS polyclonal antibody (1:100, Thermofisher Scientific, ref: PA1-036), rabbit anti-COX2 polyclonal antibody (1:100, Proteintech, ref: 12375-1-AP), rabbit anti-Arg1 polyclonal (1:100, Thermofisher Scientific, ref: PA5-85267), rabbit anti-Resistin-like Molecule α polyclonal antibody (1:100, Sigma-Aldrich, ref: AB3365P), rabbit anti-TIMP1 polyclonal antibody (1:100, Bioss, ref: BS-4600R), monoclonal mouse anti-smooth muscle actin (1:100, Dako, ref: M0851), Goat anti- PCNA Polyclonal Antibody (1:50, Invitrogen, ref: PA5-142928), Rabbit anti-ASGR1 Polyclonal Antibody (1:50, Invitrogen, ref: PA5-121041), Monoclonal rat Anti-Endomucin antibody (1:50, Abcam, ref: ab106100), rabbit anti-CD68 Polyclonal Antibody (1:100, Invitrogen, ref: PA5-78996). Primary antibodies were revealed with Cy3-conjugated donkey-anti-rabbit IgG (1:500, Jackson ImmunoResearch Laboratories, ref: 711-167-003), Cy3-conjugated donkey anti-rat IgG (1:500, Jackson ImmunoResearch Laboratories, ref: 712-165-150), donkey-anti-mouse IgG Alexa Fluor 647 (1:500, Thermofisher Scientific, ref: A31571), donkey-anti-rabbit IgG Alexa Fluor 594 (1:500, Jackson ImmunoResearch Laboratories, ref: 711-585-152), Donkey anti-Rabbit IgG Alexa Fluor 488 (1:500, Invitrogen, ref: A-21206), Donkey anti-Rat IgG Alexa Fluor Plus 488 (1:500, Invitrogen, ref: A48269) or Cy3 Donkey Anti-Goat IgG (1:500, Jackson ImmunoResearch Laboratories, ref: 705-165-147) incubated for 1h at room temperature. The presence of mannose receptor, Ly6C, PCNA, COX2, iNOS, Arginase, Resistin-like Molecule α, TIMP1 or anti-smooth muscle actin, ASGPR, endomucin and CD68 was visualized with an epifluorescence microscope. DAPI (Vectashield, Vector laboratories) was used to counterstain cell nuclei. Images were processed by computer-assisted background subtraction (low levels of staining detection, noise and background). Negative controls of immunofluorescence staining were obtained with the

incubation of liver sections with the corresponding Alexa Fluor 594 secondary antibody without the incubation of the primary antibody.

Fibrosis quantification

Liver was excised and tissue was washed with PBS and fixed with 10% buffered formaldehyde solution for 24h. Afterwards, the tissue was embedded using paraffin. Before staining, paraffin was removed using xylene, ethanol, and deionized water. Liver sections (4 µm) were stained in 0.1% Sirius Red F3B (Sigma) with saturated picric acid (Sigma). Relative fibrosis area (expressed as a percentage of total liver area) was analyzed in 20 fields of Sirius red-stained liver sections per animal using the morphometry software ImageJ v 1.44. To evaluate the relative fibrosis area, the measured collagen area was divided by the net field area and then multiplied by 100. From each animal analyzed, the amount of fibrosis as percentage was measured and the average value presented.

Hydroxyproline measurement in liver

Liver hydroxyproline content was measured following the manufacturer's protocol (Hydroxyproline Assay Kit, Sigma-Aldrich). Briefly, 10 mg of liver tissue was homogenized in distilled water, mixed with an equal volume of 10 M concentrated sodium hydroxide, and incubated at 120°C for 1 h. After alkaline hydrolysis, the samples were neutralized, oxidized, and then treated with 4-dimethylaminobenzaldehyde (DMAB) solution. Sample absorbance was measured at 560 nm in duplicate. Hydroxyproline content was expressed at microgram of hydroxyproline per gram liver. Liver protein content was measured using BCA assay kit (Thermo Fisher Scientific Inc).

Gene expression assay with Real-Time PCR

Total RNA from liver was extracted using commercially available kits: RNeasy (Gibco-Invitrogen). A 0.5 µg aliquot of total RNA was reverse transcribed using a complementary DNA synthesis kit (High-Capacity cDNA Reverse Transcription Kit, Applied Biosystems). Primers and probes for gene expression assays (Applied Biosystems) were selected as follows: *RNF41* (Taqman assay reference from Applied Biosystems: Human: Hs01086974_m1; Mouse: Mm01159897_m1), *USP8* (Human: Hs00987105_g1; Mouse: Mm00451077_m1), *IGF-1* (Mm00439560_m1), *HGF* (Mm01135184_m1), *TIMP1* (Human: Hs01092512_g1; Mouse:

Mm01341360_g1), *ACTA2* (*α-SMA*, Human: Hs00426835_g1; Mouse: Mm01204962_gH), *COL1A1* (Human: Hs00164004_m1; Mouse: Mm00801666_g1), *OSM* (Mm01193966_m1), *PDGF-BB* (Mm00440677_m1), *TGF-β* (Mm01178820_m1), *MMP-9* (Mm00442991_m1), *IL-10* (Mm00439614_m1), *CD36* (Mm00432403_m1), *NOS2* (Mm00440502_m1), *COX-2* (Mm00478374_m1), *IL1-β* (Mm00434228_m1), *ARG-1* (Mm00475988_m1), *MRC1* (Mm00485148_m1), *RETNLA* (Mm00445109_m1), *CYP2B9* (Mm00657910_m1) and mouse hypoxanthine phosphoribosyl transferase (*HPRT*, Mm03024075_m1) and human glyceraldehyde-3-phosphate dehydrogenase (*GAPDH*, Hs02786624_g1), used as endogenous standards. Expression assays were designed using the Taqman Gene Expression assay software (Applied Biosystems). Real-time quantitative PCR was analyzed in duplicate and performed with a Lightcycler-480 II (Roche Diagnostics). A 10 µl aliquot of the total volume reaction of diluted 1:8 cDNA, Taqman probe and primers and FastStart TaqMan Master (Applied Biosystems) were used in each PCR. The fluorescence signal was captured during each of the 45 cycles (denaturing 10s at 95 ºC, annealing 15s at 60 ºC and extension 20s at 72 ºC). Water was used as a negative control. Relative quantification was calculated using the comparative threshold cycle (CT), which is inversely related to the abundance of mRNA transcripts in the initial sample. The mean CT of duplicate measurements was used to calculate ΔCT as the difference in CT for target and reference. The relative quantity of the product was expressed as fold induction of the target gene compared with the control primers according to the formula $2^{-\Delta\Delta CT}$, where ΔΔCT represents ΔCT values normalized with the mean ΔCT of control samples.

Supplementary figures

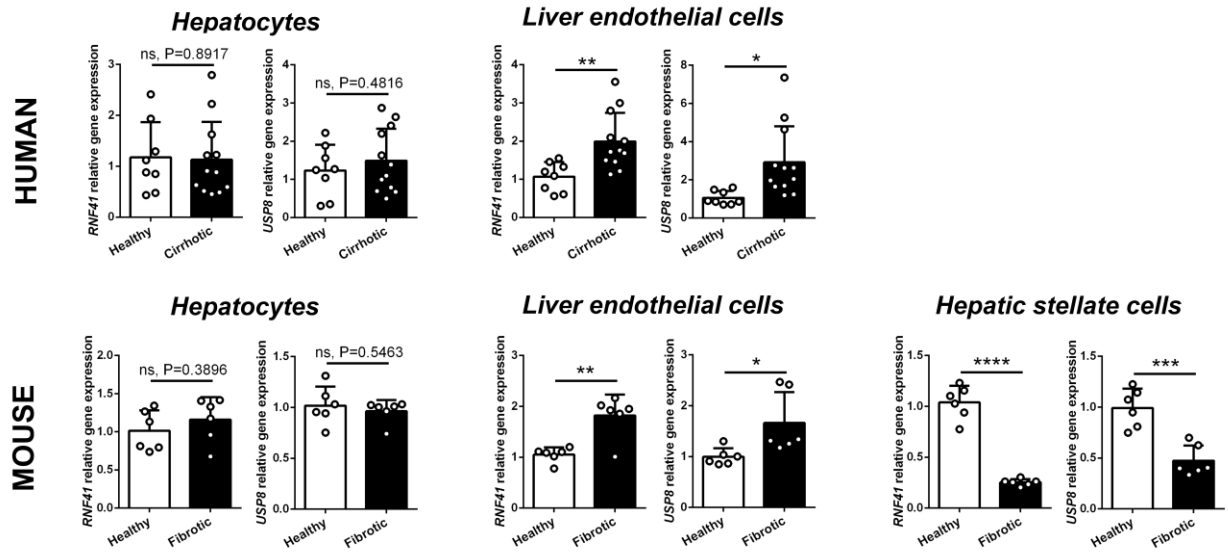

Fig. S1. *RNF41* and its stabilizer *USP8* gene expression in hepatic cells isolated from human and mouse. *RNF41* and *USP8* gene expression in hepatocytes and liver endothelial cells from patients with liver cirrhosis (n=12) and healthy subjects (n=8); and *RNF41* and *USP8* gene expression in hepatocytes, liver endothelial cells and hepatic stellate cells isolated from the liver of healthy and fibrotic mice (n=6 per group). * indicates $P \leq 0.05$, ** indicates $P \leq 0.01$, *** indicates $P \leq 0.001$, **** indicates $P \leq 0.0001$ using a Student's t-test. Data is shown as mean ± S.D.

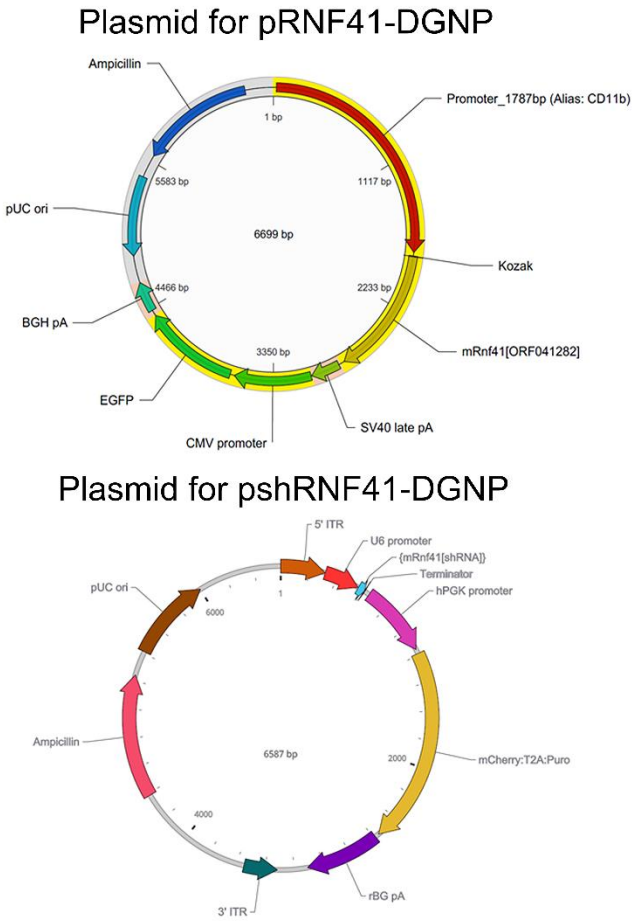

Fig. S2. Structure of pRNF41 and pshRNF41 plasmids.

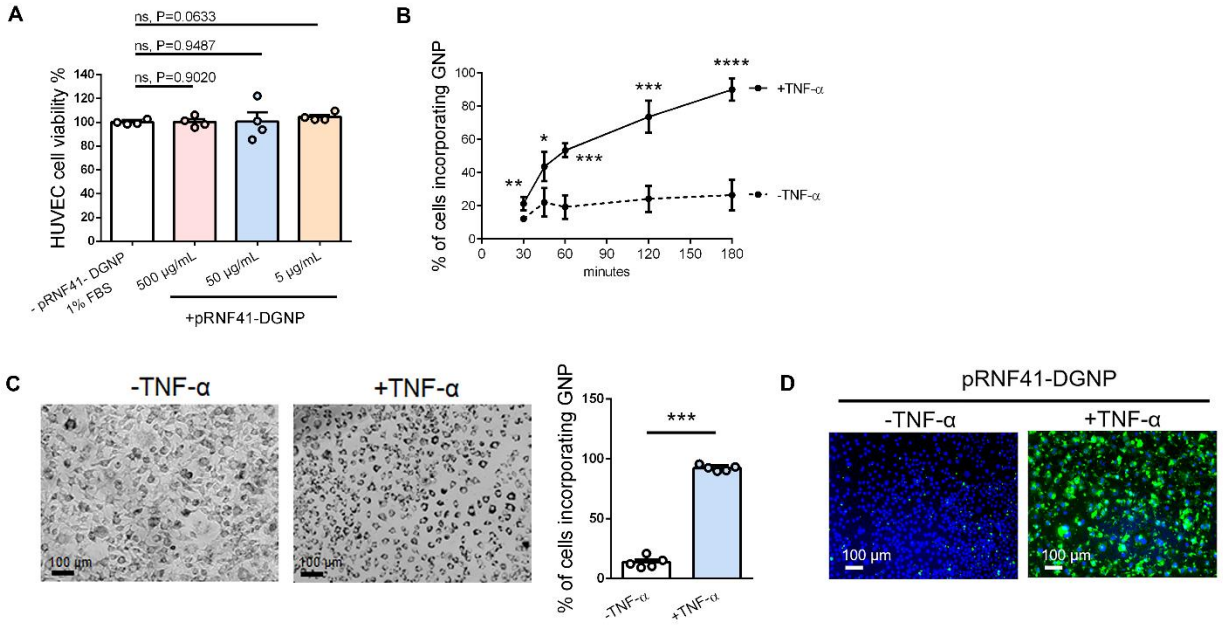

Fig. S3. Toxicity and uptake of plasmid-dendrimer graphite nanoparticles. **(A)** HUVEC viability quantified by MTS in the presence of pRNF41-dendrimer-graphite nanoparticles at concentrations from 5 to 500 µg/mL at 24h (n=4). No significant differences (ns) observed using Student's t-test compared to non-treated control. **(B)** Uptake kinetics in RAW 264.7 macrophages of pRNF41-DGNP in the presence or absence of TNF-α (n=4). * indicates $P \leq 0.05$, ** indicates $P \leq 0.01$, *** indicates $P \leq 0.001$ **** indicates $P \leq 0.0001$ vs. macrophages without TNF-α at the same time point using Student's t-test. **(C)** Uptake percentage in RAW 264.7 macrophages of pRNF41-DGNP at 24h (n=4). *** indicates $P \leq 0.001$ using a Student's t-test. **(D)** Plasmid transfection and expression efficiency highlighted by the presence of high levels of RAW 264.7 macrophage intracellular EGFP in most of cells after 3 days of incubation in TNF-α presence. Data is shown as mean ± S.D.

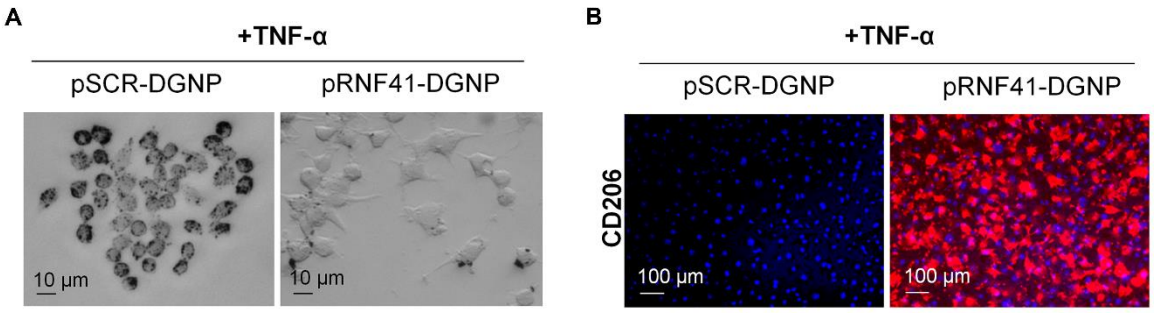

Fig. S4. Macrophage morphology and phenotype switch after pRNF41-DGNP treatment with TNF-α stimulation. (A) Cell morphology of RAW 264.7 macrophage treated with TNF-α and dendrimer-graphite nanoparticles linked to plasmids (pSCR or pRNF41), and observed using light microscopy. **(B)** Immunofluorescence staining for CD206 in RAW 264.7 macrophages treated with TNF-α and dendrimer-graphite nanoparticles linked to plasmids (pSCR or pRNF41).

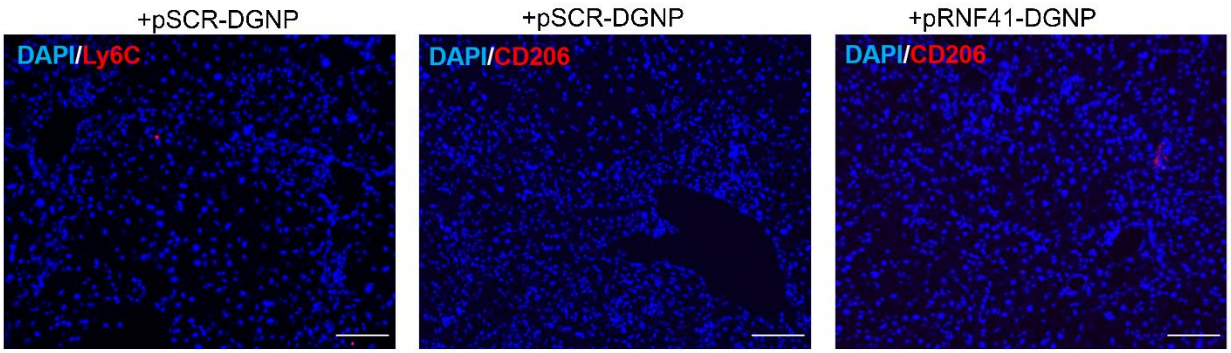

Fig. S5. Negative controls for immunofluorescence stainings. Ly6C and CD206 immunofluorescence staining negative controls in the liver of fibrotic mice treated with dendrimer-graphite nanoparticles linked to pSCR or pRNF41 for images found in Fig. 3. Scale bar: 200 µm.

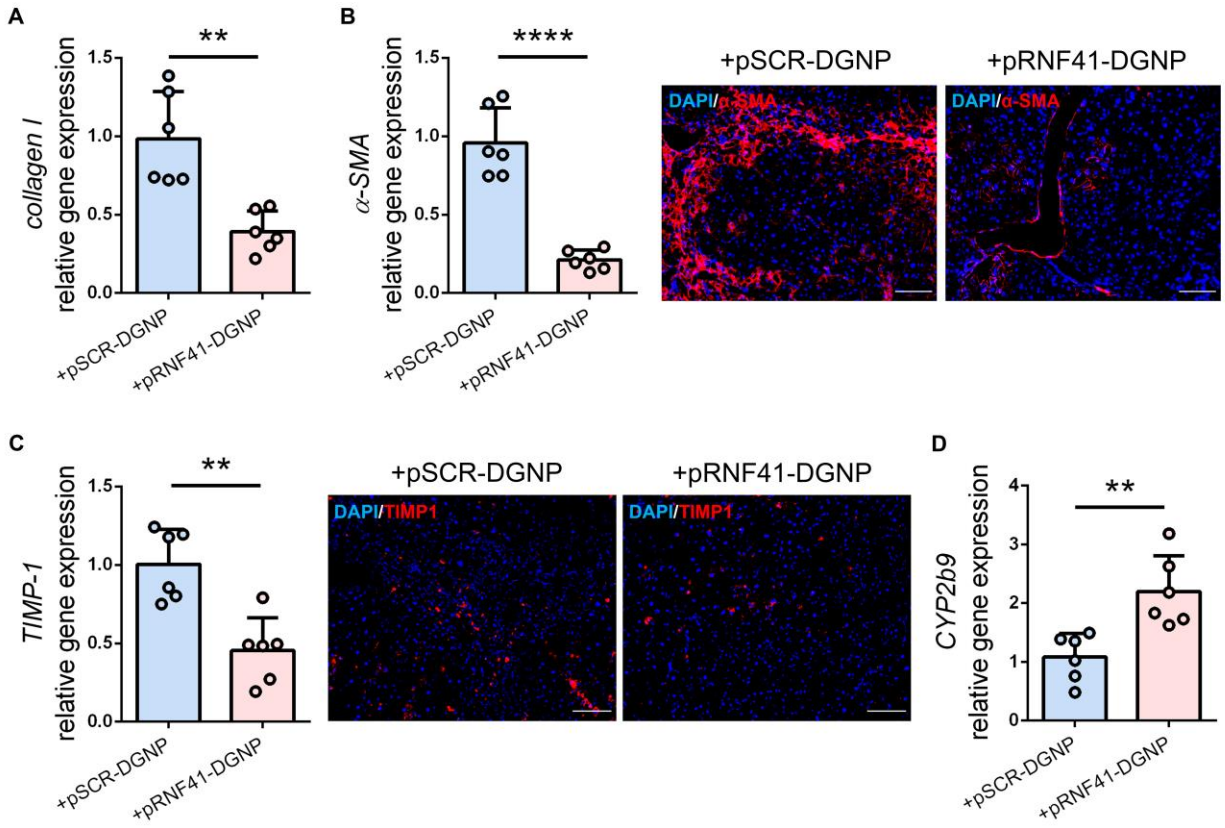

Fig. S6. Hepatic stellate cell inactivation by the treatment with pRNF41-dendrimer-graphite nanoparticles in fibrotic mice. (A) *Collagen I* relative gene expression, **(B)** *α-SMA* relative gene expression and immunofluorescence staining and **(C)** Tissue inhibitor of metalloproteinases-1 ***(****TIMP-1)* relative gene expression and immunofluorescence staining in the liver of fibrotic mice treated with dendrimer-graphite nanoparticles linked to plasmids (pSCR or pRNF41). **(D)** *CYP2B9* relative gene expression in the liver of fibrotic mice treated with dendrimer-graphite nanoparticles linked to plasmids (pSCR or pRNF41). n=6 per group of animals. ** indicates $P \leq 0.01$, **** indicates $P \leq 0.0001$ using a Student's t-test. Data is shown as mean ± S.D. Scale bar: 150 µm.

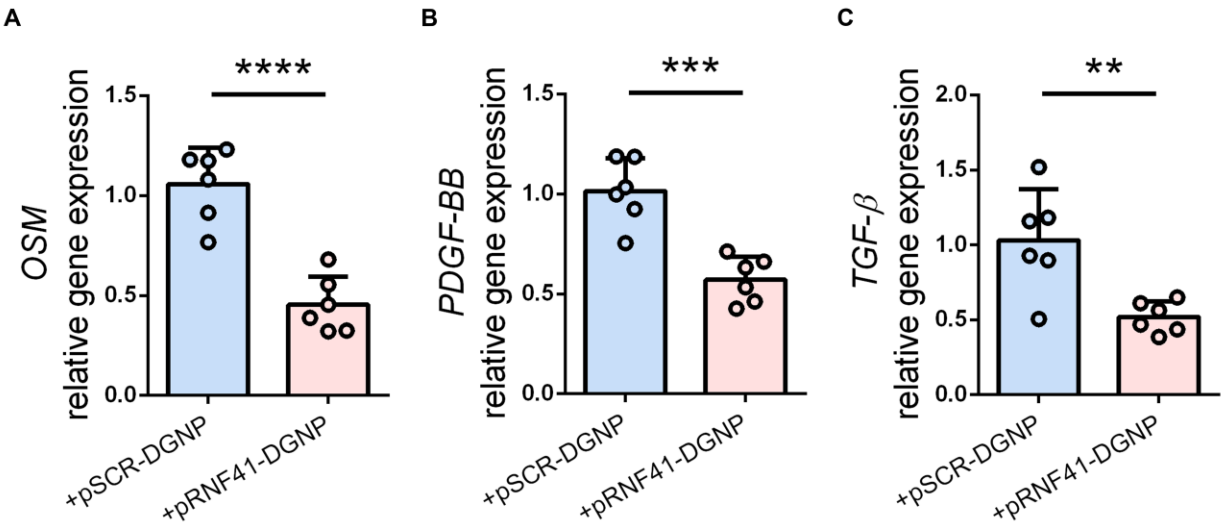

Fig. S7. Therapy with pRNF41-dendrimer-graphite reduces the relative gene expression of macrophage-derived activators of hepatic stellate cells in fibrotic mice. (A) *OSM,* **(B)** *PDGF-BB,* and **(C)** *TGF-β* relative gene expression in the liver of fibrotic mice treated with dendrimer-graphite nanoparticles linked to plasmids (pSCR or pRNF41). n=6 per group of animals. ** indicates $P \leq 0.01$, *** indicates $P \leq 0.001$, **** indicates $P \leq 0.0001$ using a Student's t-test. Data is shown as mean ± S.D.

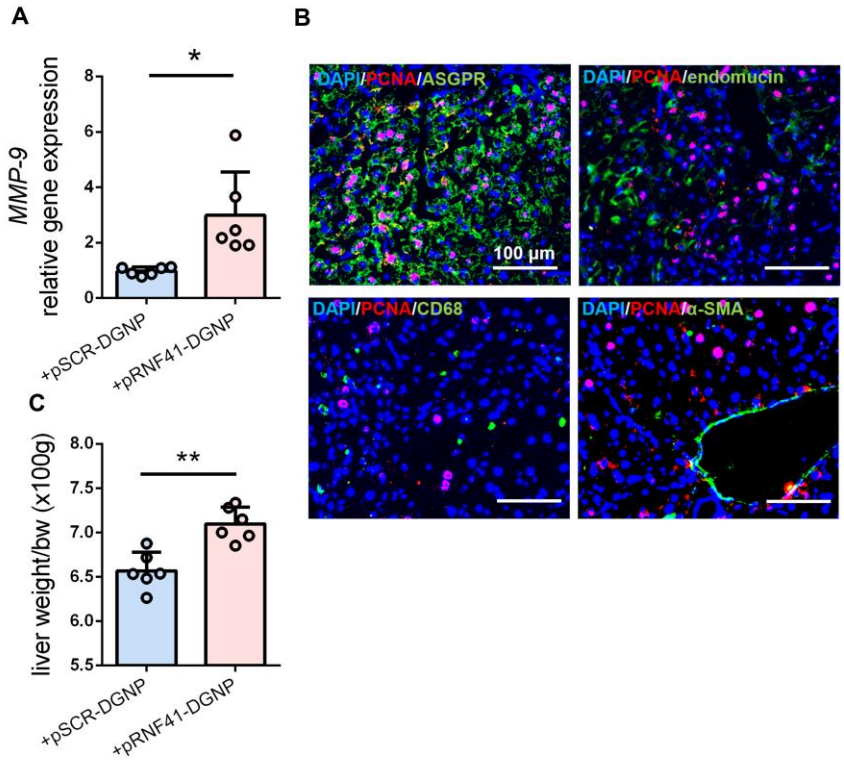

Fig. S8. The treatment with pRNF41-dendrimer-graphite nanoparticles activates the gene expression of MMP-9 and regenerates liver mass in fibrotic mice. (A) Metalloproteinase 9 *(MMP-9)* relative gene expression in the liver of fibrotic mice treated with dendrimer-graphite nanoparticles linked to plasmids (pSCR or pRNF41). **(B)** Immunofluorescence co-staining of PCNA-positive cells and individual hepatic cellular markers (asialoglycoprotein receptor (ASGPR) for hepatocytes, endomucin for liver sinusoidal endothelial cells, CD68 for macrophages and alpha smooth muscle actin (α-SMA) for hepatic stellate cells) in the liver of fibrotic mice treated with dendrimer-graphite nanoparticles linked to pRNF41. **(C)** Liver restoration rate in fibrotic mice treated with dendrimer-graphite nanoparticles linked to plasmids (pSCR or pRNF41). For a and c, n=6 per group of animals. * indicates $P \leq 0.05$, ** indicates $P \leq 0.01$ using a Student's t-test. Data is shown as mean ± S.D.

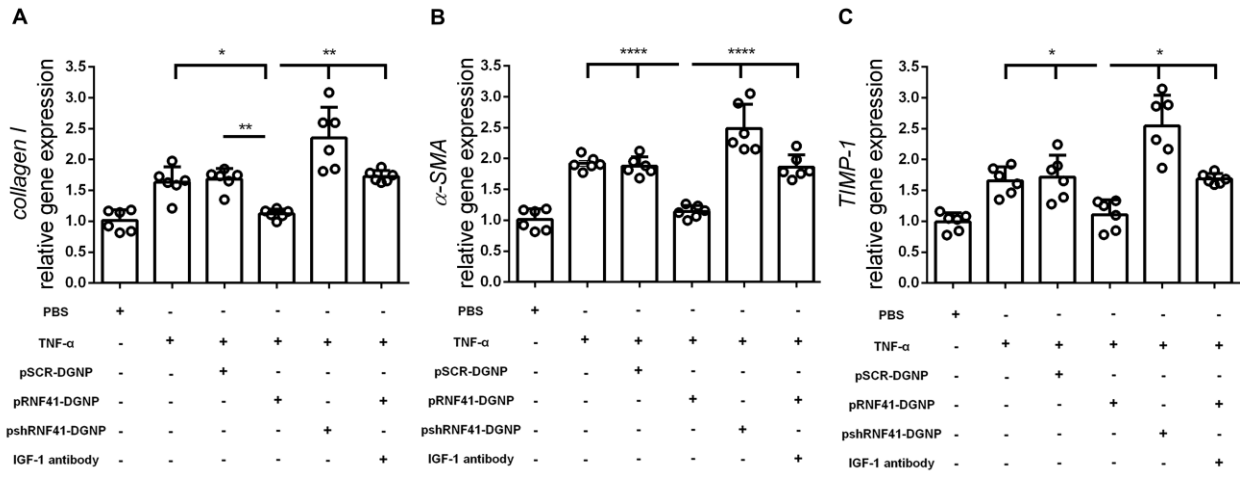

Fig. S9. IGF-1 released by RNF41-activated macrophages reduces pro-fibrogenic activation of LX-2 human hepatic stellate cells. (A) *Collagen I,* **(B)** *α-SMA,* and **(C)** Tissue inhibitor of metalloproteinases-1 *(TIMP-1)* relative gene expression in LX-2 cells treated 24 h with conditioned media from RAW 264.7 cultures treated with FBS, TNF-α, dendrimer-graphite nanoparticles linked to plasmids (pSCR, pRNF41, or pshRNF41) or IGF-1 antibody for 3 days. * indicates $P \leq 0.05$; ** indicates $P \leq 0.01$, **** indicates $P \leq 0.0001$ using a one-way analysis of variance (ANOVA) with the posthoc Newman-Keuls test. Experiments were performed in sextuplicate. Data is shown as mean ± S.D.

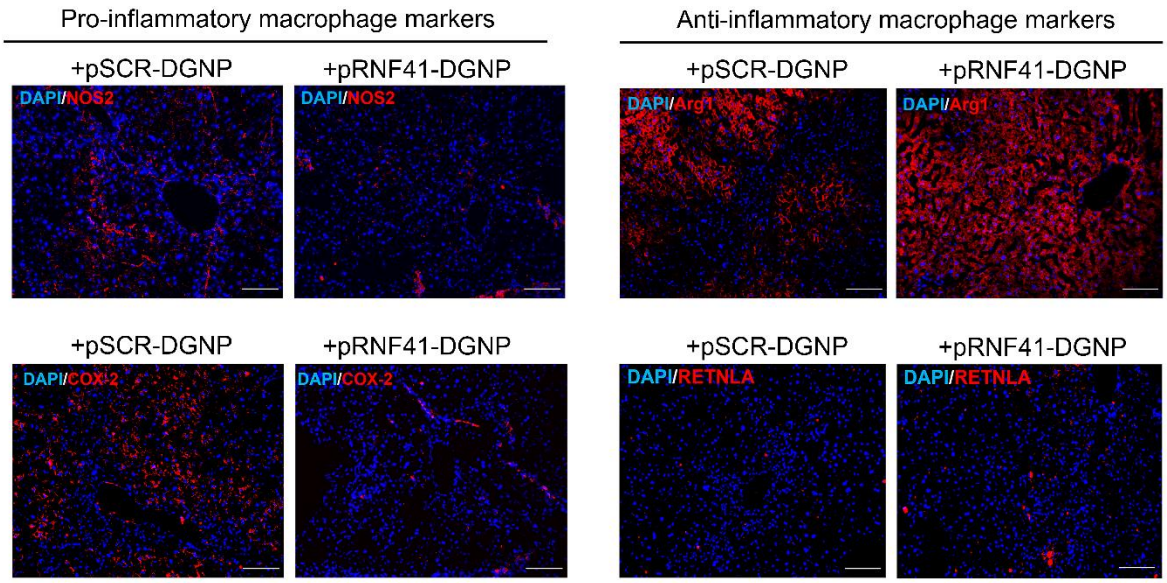

Fig. S10. Immunofluorescent staining of hepatic pro-inflammatory and anti-inflammatory markers. Pro-inflammatory macrophage marker (NOS2 and COX-2) and anti-inflammatory macrophage marker (Arg1 and RETNLA) immunofluorescence staining in the liver of fibrotic mice treated with dendrimer-graphite nanoparticles linked to plasmids (pSCR or pRNF41). Scale bar: 150 μm.

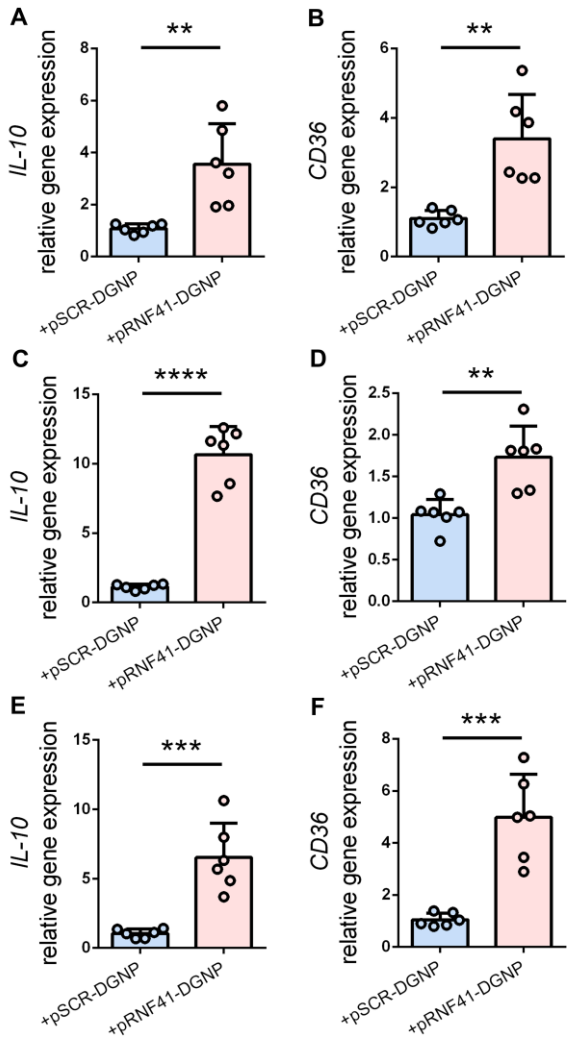

Fig. S11. The treatment with pRNF41-dendrimer-graphite nanoparticles activates the expression of the downstream PPAR-γ genes *IL-10* and *CD36* in the liver. (A) *IL-10* and **(B)** *CD36* relative gene expression in the liver of fibrotic mice treated with dendrimer-graphite nanoparticles linked to plasmids (pSCR or pRNF41). **(C)** *IL-10* and **(D)** *CD36* relative gene expression in the liver of healthy mice undergoing 70% hepatectomy and treated with dendrimer-graphite nanoparticles linked to plasmids (pSCR or pRNF41). **(E)** *IL-10* and **(F)** *CD36* relative gene expression in the liver of fibrotic mice undergoing 40% hepatectomy and treated with dendrimer-graphite nanoparticles linked to plasmids (pSCR or pRNF41). n=6 per group of animals. ** indicates $P \leq 0.01$, *** indicates $P \leq 0.001$, **** indicates $P \leq 0.001$ using a Student's t-test. Data is shown as mean ± S.D.

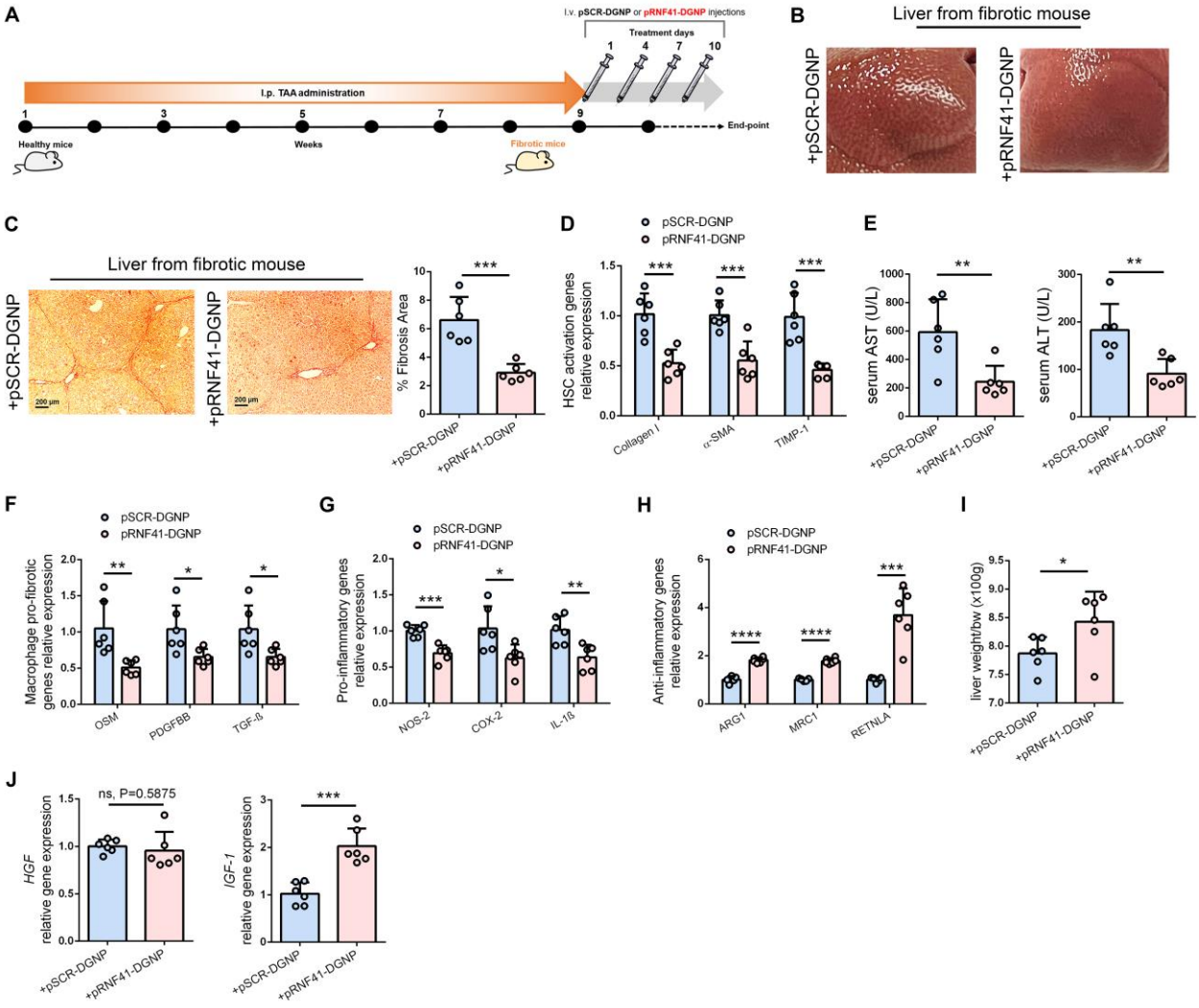

Fig. S12. ***RNF41*** **gene therapy in macrophages located into the fibrotic liver of TAA-induced fibrotic mice orchestrates fibrosis and inflammation regression, and reduction of hepatic injury. (A)** Schematic figure about time points of fibrosis induction with TAA and plasmid-linked (scrambled, pSCR or expressing RNF41, pRNF41) dendrimer-graphite nanoparticle administration. **(B)** Macroscopic aspect of fibrotic liver changing from micronodular fibrotic liver to an apparently low fibrotic liver when treated with pRNF41-DGNP. **(C)** Sirius Red staining and quantification of fibrosis area in the liver of fibrotic mice treated with dendrimer-graphite nanoparticles linked to plasmids (pSCR or pRNF41). **(D)** Expression of genes related to hepatic stellate cell (HSC) activation in the liver of fibrotic mice treated with dendrimer-graphite nanoparticles linked to plasmids (pSCR or pRNF41). **(E)** Serum parameters of liver injury in fibrotic mice treated with dendrimer-graphite nanoparticles linked to plasmids (pSCR or pRNF41). **(F)** Gene expression of pro-fibrogenic agents produced by macrophages in the liver of fibrotic

mice treated with dendrimer-graphite nanoparticles linked to plasmids (pSCR or pRNF41). **(G)** Expression of inflammatory macrophage genes in the liver of fibrotic mice treated with dendrimer-graphite nanoparticles linked to plasmids (pSCR or pRNF41). **(H)** Expression of anti-inflammatory macrophage genes in the liver of fibrotic mice treated with dendrimer-graphite nanoparticles linked to plasmids (pSCR or pRNF41). **(I)** Liver restoration rate in fibrotic mice treated with dendrimer-graphite nanoparticles linked to plasmids (pSCR or pRNF41). **(J)** Hepatic expression of hepatocyte growth factor (*HGF*) and insulin-like growth factor 1 (*IGF-1*) in fibrotic mice treated with dendrimer-graphite nanoparticles linked to plasmids (pSCR or pRNF41). n=6 per group of animals. For c, d, e, f, g, h and I * indicates $P \leq 0.05$, ** indicates $P \leq 0.01$, *** indicates $P \leq 0.001$, **** indicates $P \leq 0.0001$ using a Student's t-test.

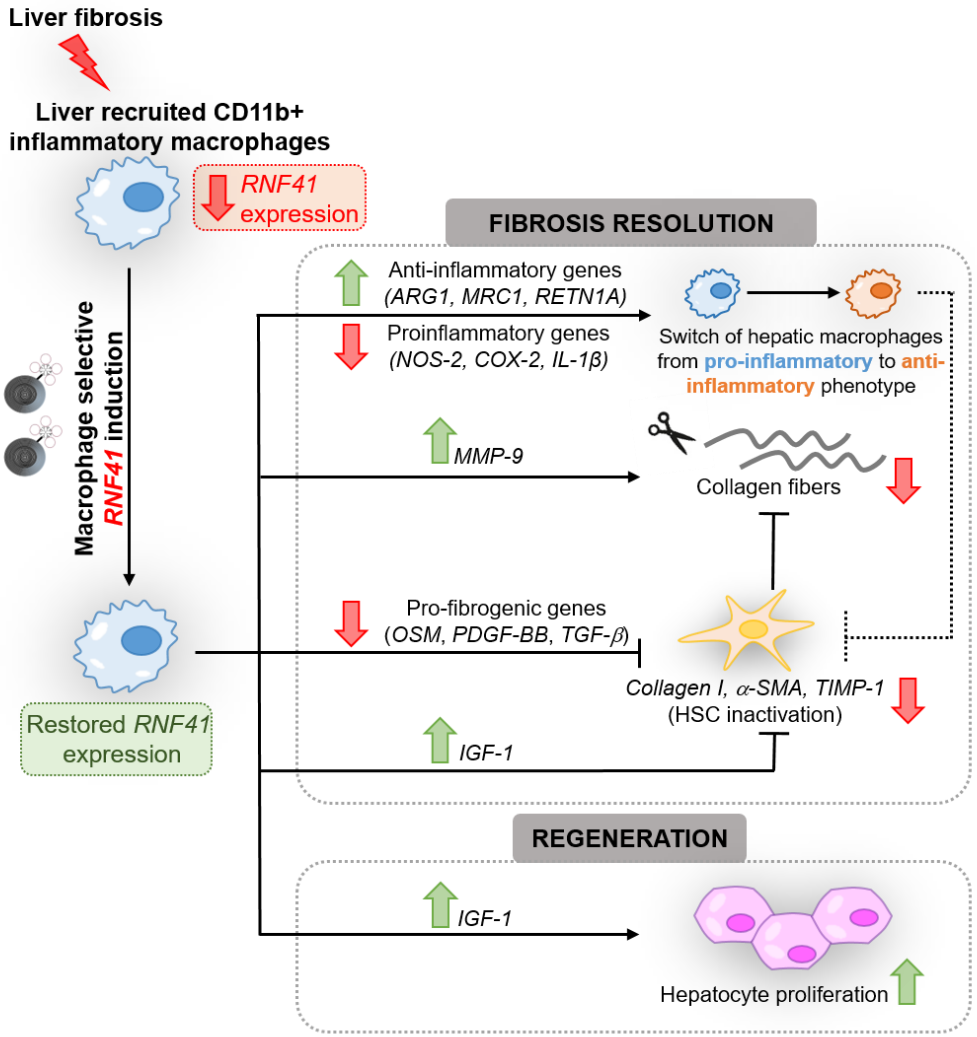

Fig. S13. Summary illustration of the heterogeneous impacts of macrophage *RNF41* restoration on liver fibrosis and regeneration.

Supplementary tables

Table S1: Demographic and baseline characteristics of study participants.

Variables	Cirrhotic n=12	Healthy n=8
Age (years)	58.7 ± 6.1	56.4 ± 19.3
Gender		
Male	9 (75)	3 (37.5)
Female	3 (25)	5 (32.5)
BMI (kg/m^2)	26.9 ± 3	24.5 ± 2.1
Etiology of liver disease		
Alcoholic	7 (58.3)	
Alcoholic + MAFLD	1 (8.3)	
Alcoholic + NASH	2 (16.7)	
PBC	1 (8.3)	
Alcoholic + HCV	1 (8.3)	
Child-Pugh Score		
A	1 (8.3)	
B	3 (25)	
C	8 (66.7)	
MELD score	20.7 ± 5.1	
Cirrhosis duration (years)	4.3 ± 5.8	

Data is shown as Mean ± S.D., or Number of Participants (Percentage, %).

BMI: Body Mass Index; MAFLD: Metabolic associated fatty liver disease; NASH: Non-Alcoholic Steatohepatitis; PBC: Primary Biliary Cirrhosis; HCV: Hepatitis C Virus; MELD: Model for End-Stage Liver Disease

Table S2: Bioinformatic analyses of *RNF41* expression in mouse and human databases.

Bioinformatic source	Species	Tissue or cell type	Disease	*RNF41* Expression levels	Reference/ID
Single-Cell Expression atlas (EBI) Baseline	Human	Liver	Normal	Below cutoff	Kim MS et al. 2014
	Mouse	Kupffer Cell	Normal	12 TPM	Lavin Y et al. 2014
				295 PPB	Azimizar SB et al. 2014
Single-Cell Expression atlas (EBI) Differential	Human	Mononuclear cells	Infected by F. Tularensis	-1.4 Fc	Butchar JP et al. 2008
	Mouse	Liver	Hepatitis (Cnot1 liver-specific KO)	-1.7 Fc	Suzuki T et al. 2020
NCBI Genes	Human	Liver	Hepatitis B virus	Lower levels	Cao K et al. 2016
	Mouse	Isolated Microglia	Inflamed with LPS	Lower levels	Zhu L et al. 2015
GEO profiles	Human	Myelogenous leukemia cell line THP-1	Inflamed with LPS	Value reduction: 95,279	ID: 76881910
	Mouse	Wild type Macrophage	Inflamed with LPS	Value reduction: 58,789	ID: 44617209
Specific Single-cell RNA-seq (Bulk data)	Human	Cycling Scar-associated macrophages	Liver cirrhosis	Reduced expression	Ramachandran P et al. 2019

TPM: transcript per million; PPB: parts per billion; F. Tularensis: Francisella tularensis; Fc: Log2-fold change; Cnot1: CCR4-NOT Transcription Complex Subunit 1; KO: Knock out; NCBI: National Center for Biotechnology Information; LPS: Lipopolysaccharide; GEO: Gene Expression Omnibus.

The online material for this manuscript contains the following Excel file:

Data file S1. Raw data from figures.